



CrossMark  
click for updates

Cite this: *RSC Adv.*, 2016, 6, 16941

# Impact of carbon nanotubes on the mobility of sulfonamide antibiotics in sediments in the Xiangjiang River

Chang Su,<sup>ab</sup> Guang-Ming Zeng,<sup>\*ab</sup> Ji-Lai Gong,<sup>\*ab</sup> Chun-Ping Yang,<sup>ab</sup> Jia Wan,<sup>ab</sup> Liang Hu,<sup>ab</sup> Shan-Shan Hua<sup>ab</sup> and Yan-Yan Guo<sup>ab</sup>

Manufactured in numerous factories, and contained in various consumer products, carbon nanotubes (CNTs) and sulfonamide antibiotics (SAs) may be released into the environment by many pathways. The sorption behavior of CNTs on SAs may increase the environmental and health risks when exposed to SAs–CNTs composites. In this study, we investigated the mobility of SAs in sediment columns in the presence/absence of CNTs. Three kinds of SAs (sulfamethoxazole, sulfapyridine, and sulfadiazine) and two kinds of CNTs (multi-walled carbon nanotubes, MWCNTs and single-walled carbon nanotubes, SWCNTs) in sediments from the Xiangjiang River were investigated in this study. The results showed that the SAs were of high mobility in sediment columns. However, CNTs with a concentration of 4.8 mg g<sup>−1</sup> in the sediment could dramatically retain SAs, which might be due to the limited transport of CNTs and their high adsorption capacities of SAs. The percentage of SAs retention in sediment became higher when CNTs existed in the inflow, suggesting that a strong CNTs-associated SAs reaction might occur in the sediment. The findings in this study indicated that CNTs in the sediment environment or river system can reduce the mobility of SAs, which should be taken into account when evaluating the potential environmental risks of SAs and CNTs.

Received 27th November 2015  
Accepted 4th February 2016

DOI: 10.1039/c5ra25201f

www.rsc.org/advances

## 1. Introduction

Carbon nanotubes (CNTs), which are tubular nanoparticles with nanoscale diameters and micro-scale lengths, contain a single layer cylindrical graphite sheet (single-walled carbon nanotubes, SWCNTs) or multi-layers cylindrical graphite sheets (multi-walled carbon nanotubes, MWCNTs).<sup>1,2</sup> CNTs are of great importance in enhancing the sensitivity and electro catalytic activity of the corresponding sensor devices.<sup>3</sup> Owing to their large specific surface area, small size, and layered structures, CNTs have been proven to be superior adsorbents for removing many kinds of organic and inorganic contaminants.<sup>4–7</sup> On account of these special properties, CNTs are considered as one of the most promising materials, with the applications in many fields, including electronics, pharmaceuticals and environmental science.<sup>8,9</sup> With a rapid commercialization, their increasing release is inevitable through manufacture process, abrasion of materials containing CNTs, accidental release during transport, and landfills and wastewater treatment.<sup>10–12</sup> Simultaneously, CNTs rapid equilibrium rates and high adsorption capacity for environmental pollutants might enhance the eco-

toxicity of coexisting contaminants, which made CNTs an increasingly important environmental contaminant.<sup>7,13</sup> Therefore, a thorough understanding of the environmental behavior of CNTs is essential to reasonably evaluate their potential hazard in the environment.

Lots of findings indicated that CNTs could have an impact on the mobility and fate of other contaminants. Hofmann and von der Kammer theoretically analyzed the transport of hydrophobic organic contaminants (HOCs) in porous media by carbonaceous engineered nanoparticles (ENPs), reporting that carbonaceous ENPs may act as carriers for contaminants.<sup>14</sup> Wang *et al.* studied the influence of CNTs on transport of nano-TiO<sub>2</sub> in variable situations, finding that multi-walled carbon nanotubes could facilitate the transport of nano-TiO<sub>2</sub> at pH 7 while it showed different effects in different ionic strengths at pH 5.<sup>15</sup> Moreover, they also conducted experiments to explore the mobility research in real soil system. Kasel *et al.* made a conclusion that the soils may act as a strong sink for MWCNTs which limited the potential groundwater contamination.<sup>12</sup> Lu *et al.* also found that soil texture rather than soil organic matter (SOM) controlled the CNTs mobility through Pearson correlation analyses.<sup>16</sup> CNTs also influenced the transport of other contaminants. Li *et al.* demonstrated that the CNTs with concentration of 5 mg g<sup>−1</sup> could significantly retain polycyclic aromatic hydrocarbon (PAHs) in soil.<sup>17</sup> Fang *et al.* showed that the effects of MWCNTs on the mobility of phenanthrene in real

<sup>a</sup>College of Environmental Science and Engineering, Hunan University, Changsha 410082, P. R. China. E-mail: zgming@hnu.edu.cn; jilaigong@gmail.com; Fax: +86 731 88822829; Tel: +86 731 88822829

<sup>b</sup>Key Laboratory of Environmental Biology and Pollution Control (Hunan University), Ministry of Education, Changsha 410082, P.R. China

soil was correlated to the average soil particle diameters, soil sand contents and soil clay contents.<sup>18</sup>

Sulfonamide antibiotics (SAs) are a kind of antibiotics which are widely used as human and veterinary pharmaceuticals to promote infectious disease therapy and growth.<sup>19</sup> The pathways of SAs entering environmental system include pharmaceutical manufacturing, livestock treatment and medical waste disposal.<sup>20,21</sup> However, SAs are not removable through the typical sewage treatment plants and can bioaccumulate up the food chains.<sup>20,22</sup> Surface runoff and leaching were two important transport pathways for the fate of SAs.<sup>23</sup> These facts led to a detection of SAs in aquatic environments around the world, including coastal wetlands, freshwater streams and estuarine sediments.<sup>22,24,25</sup> SAs could induce antibiotic resistance, trigger acute and chronic adverse effects, and enhance toxic effects to organisms while simultaneously multiple exposure.<sup>26–28</sup> The protection of sediment and groundwater quality from contamination of leached SAs is of great priority for public and environmental health.<sup>29</sup>

In recent years, many researches have been done to investigate the adsorption property of CNTs on SAs. It has been reported that the adsorption isotherms for SAs on both MWCNTs and SWCNTs were nonlinear and could be described well with the Freundlich isotherm model, meanwhile, the adsorption efficiency of SWCNTs was better than that of MWCNTs.<sup>30</sup> The adsorption behavior of sulfamethoxazole, which was a kind of SAs, on CNTs was controlled by CNTs properties, such as surface areas, diameters, and functional groups.<sup>31</sup> Evidences have shown that both electrostatic effect and hydrophobic interaction could affect the SAs adsorption on CNTs. With the addition of cations/anions, both increasement and decrease of SAs adsorption could be observed, and the balance of which mostly depended on environmental factors.<sup>32</sup> Ji *et al.* also observed the effects of pH on the adsorption of SAs and suggested that the adsorption behavior was much stronger for the protonated neutral sulfonamide than the deprotonated anionic counterpart.<sup>33</sup> In general, CNTs showed good adsorption coefficients for SAs, its adsorption coefficients were two orders of magnitude higher than that of soil, sediment, and sludge. Therefore, CNTs may dominate SAs behavior and its environmental risks, especially in polluted water and solid waste during plant treatment.<sup>31</sup> The suspended CNTs which had larger exposed surface area may show more advantages in enhancing the mobility of the nanoparticles due to the increasing possibility of exposure to organic contaminants when compared to the aggregated CNTs.<sup>34</sup> Moreover, Tian *et al.* demonstrated that fixed-bed columns packed with CNTs could be efficiently used to remove SAs from water. A broad range of factors, such as CNTs incorporation method, solution pH, bed depth, adsorbent dosage, adsorbate initial concentration, and flow rate, might also have an impact on removal of SAs.<sup>29</sup> These studies made a foundation of CNTs–SAs transport research. However, no prior report on the transport of SAs in real sediment environment in the absence/presence of CNTs was documented.

To better understand and assess the future risk, there is a need to study the effects of CNTs on the transport and deposition of SAs in underground environment. In this study, the repacked

sediments in Xiangjiang River, central-south China were used to evaluate the SAs migration potential and the associated impact of CNTs–SAs in real natural sediment system. Hence, the main objectives of this study were to investigate the transport behavior of three typical SAs including sulfamethoxazole (SMX), sulfapyridine (SPY), and sulfadiazine (SDZ) in different sediment columns, and to explore how MWCNTs and SWCNTs in inflow affected the transport of SAs in sediments. The current work might contribute to a further insight into the mechanisms that drive the transport and fate of SAs associated with CNTs in sediment system. Accordingly it may generate scientific and technological advances, as well as economical benefits.

## 2. Materials and methods

### 2.1 Chemicals and reagents

SWCNTs (purity > 95%, length 5–30  $\mu\text{m}$ , outer diameter 1–2 nm, and specific surface area: 690  $\text{m}^2 \text{g}^{-1}$ ) and MWCNTs (purity > 95%, length 50  $\mu\text{m}$ , outer diameter 8–15 nm, and specific surface area: 200  $\text{m}^2 \text{g}^{-1}$ ) were purchased as powders from Chinese academy of sciences, Chengdu organic chemistry co., LTD and were used without further purification.

Sulfamethoxazole (>99%), sulfapyridine (>99%), and sulfadiazine (>99%) were obtained from Aladdin Industrial Corporation (Shanghai, China). High performance liquid chromatography (HPLC) grade methylene chloride and acetonitrile were purchased from Tedia Company, Inc. (USA). Ultrapure water (18.25 M $\Omega$ ) was prepared by an ultrapure water machine, UPT-11-40 (ULUPURE, Chengdu, China). All other chemicals used in the study were of or above analytical grade.

### 2.2 Sediments collection and pretreatment

Xiangjiang River is the largest river in Hunan Province, China. It flows from the south to north, eventually into the Dongting Lake, Yangtze River. Surface sediment samples (top 0–15 cm) were collected from five sites in December 2014. All these sites are located in Changsha reach of Xiangjiang River, Hunan province, China (Fig. 1). Three parallel sediment samples were collected from every site. Then the samples were transported within four hours to the laboratory. Sediments were air dried, cleaned up the leaves, mashed in the mortar and passed through a 0.9 mm sieve to use as experimental material. Samples for sediment properties determination work were stored at 25  $^{\circ}\text{C}$ .

The pH value of sediment was measured with a digital pH meter (water : sediments ratio of 1 : 1, v/v). SOM was determined following the procedures defined by Nelson.<sup>35</sup> Cation-exchange capacity (CEC) was calculated according to Hendershot and Liang.<sup>36,37</sup> Zeta potential of sediment was measured using a Zetasizer Nano Series Instrument (Malvern Instrument Ltd. UK). Particle size distribution (sediment texture: clay, silt and sand) was determined using a hydrometer method.<sup>38</sup> All experiments were conducted in duplicate and the average values were obtained. Measurements of parallel experiments did not show a difference larger than 5%. The analytical physical and chemical properties of sediment were given in Table 1. Sediment samples contained no detectable level of SAs.

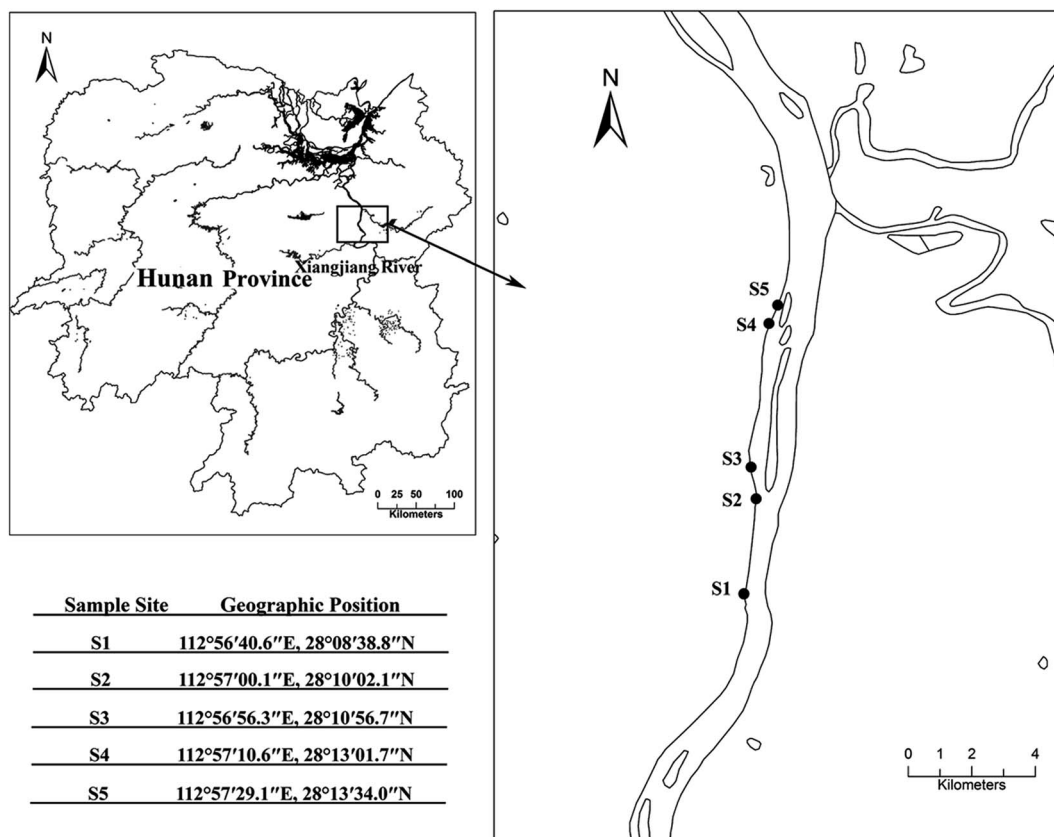


Fig. 1 Map of study area and sampling sites.

Table 1 Physical and chemical properties of the sediments

pH	CEC (cmol kg <sup>-1</sup> )	SOM (%)	Zeta potential (mV)	Texture% (v/v)		
				Clay (<2 μm)	Silt (2–50 μm)	Sand (50–900 μm)
7.29	386.7	1.9	−14.6	11.2	20.0	68.8

### 2.3 Adsorption of sulfonamide antibiotics on sediments and carbon nanotubes

The effect of contact time on the adsorption of SAs by sediments and CNTs were studied by applying 50 mL lined capped glass bottles containing 20 mg sediments and 10 mg CNTs respectively, and 30 mL of 50 mg L<sup>-1</sup> SAs. The glass bottles were in a shaker at 150 rpm, 25 ± 1 °C. Samples were taken out from different bottles at predetermined time intervals (from 6 min to 48 h), filtered with a 0.22 μm membrane and then determined.

The sorption isotherms experiments were conducted in 50 mL lined capped glass bottles by mixing 20 mg sediments and 10 mg CNTs respectively with varying concentrations (10 mg L<sup>-1</sup>, 20 mg L<sup>-1</sup>, 30 mg L<sup>-1</sup>, 40 mg L<sup>-1</sup>, and 50 mg L<sup>-1</sup>) of SAs in a shaker for 48 hours at 150 rpm, 25 ± 1 °C. The pH values of the solutions were 5.5 ± 0.2, which were measured using a digital pH meter.

### 2.4 Column experiments

**2.4.1 Column packing.** A Teflon column (20 cm long with an inner diameter of 24 mm), which had been depolished in the innerwall to make it rough to avoid the preferential flow, was used in this study. The column was equipped with a Teflon inlet at the top and a Teflon outlet at the bottom. Each type of 288 mg CNTs was mixed separately with 60 g air-dried sediments in a beaker. Then the CNTs-sediments mixture or air-dried sediments alone was uniformly packed in the column with a height of 10 cm. Glass wools were used as support at the bottom of column to prevent losses of sediments particles. Air-dried sediments alone in column was called sediment. Sediments mixed with MWCNTs or SWCNTs in column was called: MWCNTs-S or SWCNTs-S.

**2.4.2 Column leaching experiment.** The column experiments were designed based on previous studies.<sup>17,18,39</sup> The column setup consisted of a reservoir containing the inflow

solution, a peristaltic pump, a Teflon column containing the repacked sediments or CNTs-mixed sediments, and a small glass collector. Column breakthrough experiments of SAs were performed under saturated flow conditions. The columns were initially saturated with ultrapure water. Ultrapure water was added from the bottom of the column and gradually moved upwards through the entire column to remove any air pockets, and then the saturated column was leached with 100 mL ultrapure water from the top. After saturating process, the absorbance of outflow was less than 0.03 measured at 800 nm, suggesting that soil colloid in the outflow was significantly reduced.<sup>18</sup>

All the experiments were conducted at 25 °C. The initial concentration of SAs in column leaching experiments was 50 mg L<sup>-1</sup> while the CNTs in the inflow suspensions were 0.33 mg mL<sup>-1</sup>. Three different sets of column experiments were performed. The first set of experiments aimed at understanding the mobility of SAs in natural sediment and CNTs-contaminated sediment. SAs solution was pumped onto the top of the columns. In the second set of experiments, the SAs–CNTs mixture which had been mixed and shaken for three days and reached equilibrium was pumped onto the top of the sediments columns. The third set of experiments was performed with SAs solutions and CNTs powders which had not been mixed in advance. They were pumped onto the top of the sediments columns. The two sets (*i.e.* the second and third sets) of experiments were conducted to mimic the SAs–CNTs co-contaminants leaching in sediment system at two different situations. Additionally, a saturated sediments column leached with ultrapure water was used as the control. The absorbance of control column outflow at 800 nm was also measured to monitor the sediment colloid release. In all sets of experiments, the flow rate was fixed at 0.3 mL min<sup>-1</sup>. A water head of 2 cm was maintained throughout the experiment. The inflow was leached in the gravity flow. Pore volume was calculated based on volume change after water saturation. The outflow was collected at a speed of every 0.33 pore volume, and then filtered with a 0.22 µm membrane for analysis. The pH values of the outflows were 5.8 ± 0.3. At the end of the experiment, columns were cut into slices at 1.0 cm thick. 4.0 g sediments in each slice were taken out, air-dried, and then ready for extraction.

## 2.5 Analysis

All adsorption experiments and column leaching experiments were conducted in triplicate and the average values were obtained. The analysis results were reliable when repeat sample analysis error was below 5%, and the analytical precision for replicate samples was within ±5%. Standard materials (>99%) and method blank were analyzed with each sample batch. UV spectrums of SAs solutions at every 12 hours indicated that the SAs concentrations were unchanged within 7 days. Thus the degradation of SAs was negligible during the experiment period.

Concentrations of SMX, SPY and SDZ in solutions were analyzed using a UV-visible spectrophotometer (Shimadzu UV-2550) at 265 nm. The method detection limit regarding SAs was 0.012 mg L<sup>-1</sup>. The solid-phase sample extraction was

performed according to EPA method.<sup>40</sup> Concentrations of SMX, SPY and SDZ in sediment were determined by HPLC (Agilent 1100, USA) equipped with an UV-vis photodiode array detector. They were detected using a mobile phase containing acetonitrile : water (isocratic: 20 : 80, v/v; flow rate = 1.0 mL min<sup>-1</sup>). The wavelength of 265 nm was used and the HPLC column temperature was 25 °C. Retention times of SMX, SPY and SDZ were 6.02 min, 6.91 min, and 6.00 min respectively. The method detection limit regarding SAs was 0.135 µg g<sup>-1</sup>. Recovery of SAs from samples was 60 ± 10%, which was consistent with EPA method.<sup>40</sup>

## 3. Results and discussion

### 3.1 SAs adsorption onto sediments and CNTs

**3.1.1 Adsorption kinetics.** The effect of contact time on the adsorption of SAs by sediments and CNTs was shown in Fig. 2. For sediments, the adsorption behaviors toward SAs were not obvious. The adsorption rate increased slightly within 6 min and then equilibriums were almost achieved. However, the equilibrium adsorbed values of SAs on CNTs were much higher than on sediments. It was observed that a rather fast uptake of three kinds of SAs occurs during 6 min followed by a slower stage as the adsorbed amount of SAs reaches its equilibrium value with the adsorbed SMX, SPY and SDZ reaching 50.54 mg L<sup>-1</sup>, 33.89 mg L<sup>-1</sup> and 30.14 mg L<sup>-1</sup> respectively in MWCNTs adsorption. The adsorption processes of SWCNTs toward SMX and SDZ were very fast during the first 3.2 hour followed by slight increase before the equilibriums were reached at about 24 h. For SPY, the dramatically increased stage of adsorption rate extended to 6.4 hour and an apparent equilibrium was achieved at about 18 h. The strong adsorption affinity between SAs and CNTs might be owing to large specific surface areas of CNTs.

To illustrate the adsorption process and provide insights into possible reaction mechanisms, the results were fitted using a pseudo-second-order kinetic model, which can be expressed as:

$$\frac{t}{q_t} = \frac{1}{kq_e^2} + \frac{t}{q_e} \quad (1)$$

where  $k$  (g mg<sup>-1</sup> h<sup>-1</sup>) is the second-order rate constant,  $q_t$  (mg g<sup>-1</sup>) and  $q_e$  (mg g<sup>-1</sup>) represent adsorbed amount of adsorbate at any time  $t$  (h) and at equilibrium, respectively.

Table 2 listed the results of adsorption kinetics using the fittings of pseudo second-order model. It showed that the linear relationships between  $t/q_t$  and  $t$  were with very high correlation coefficients ( $R^2$ ), indicating the applicability of the pseudo second-order model to describe the adsorption process.

**3.1.2 Adsorption isotherms.** Freundlich and Langmuir models were used to determine the proper isotherm for SAs adsorption on sediments and CNTs. The equations of the Freundlich and Langmuir models can be expressed as:

$$\text{Freundlich: } Q_e = K_f C_e^n \quad (2)$$

$$\text{Langmuir: } Q_e = \frac{Q_m K_L C_e}{1 + K_L C_e} \quad (3)$$



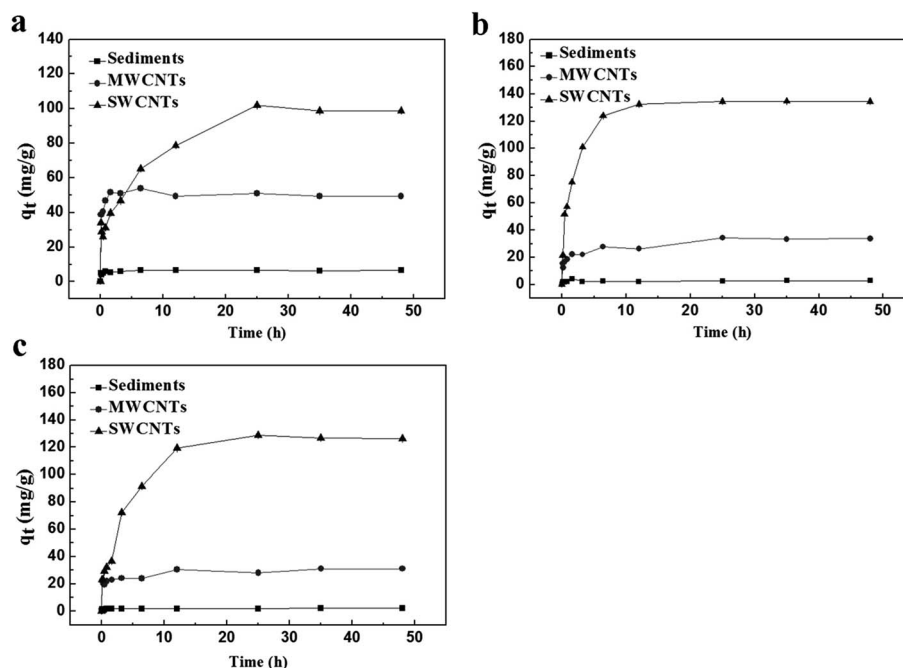


Fig. 2 Effect of contact time on the adsorption of SMX (a), SPY (b), and SDZ (c) by sediments, MWCNTs and SWCNTs.

Table 2 Kinetic parameters for SAs adsorption by sediments, MWCNTs and SWCNTs, modeled by a pseudo second-order equation

Adsorbate	Adsorbent	<i>k</i>	<i>q<sub>e,measured</sub></i>	<i>q<sub>e,calculated</sub></i>	<i>R</i> <sup>2</sup>
SMX	Sediments	2.500	6.548	6.489	0.9994
	MWCNTs	0.2915	50.54	49.50	0.9997
	SWCNTs	0.005535	99.79	103.1	0.9923
SPY	Sediments	0.6889	2.792	2.827	0.9959
	MWCNTs	0.03292	33.89	34.25	0.9960
	SWCNTs	0.009516	134.5	136.9	0.9995
SDZ	Sediments	1.079	2.117	2.143	0.9973
	MWCNTs	0.05861	30.14	30.96	0.9972
	SWCNTs	0.004443	127.3	131.5	0.9946

where  $Q_e$  ( $\text{mg g}^{-1}$ ) is the apparent solid-phase and  $C_e$  ( $\text{mg L}^{-1}$ ) is the aqueous phase equilibrium concentrations,  $K_f$  [ $(\text{mg kg}^{-1})(\text{mg L}^{-1})^{-n}$ ] is the Freundlich affinity coefficient,  $n$  (dimensionless) is the Freundlich linearity parameter,  $Q_m$  ( $\text{mg g}^{-1}$ ) is the maximum adsorption capacity, and  $K_L$  ( $\text{L mg}^{-1}$ ) is the Langmuir constant related to adsorption energy.

The results were presented in Fig. 3 and Table 3. In general, the Freundlich model was more suitable than the Langmuir isotherm for the adsorption of SAs on sediments since the correlation coefficients ( $R^2$ ) were very low ( $<0.75$ ) and the maximum adsorption capacities were illogically high in Langmuir fitting. These results indicated that the adsorption of SAs on sediments were not pure monolayer type, which were similar to the results of previous works in adsorption process of SAs on soils, sediments and biochars.<sup>31,41,42</sup>

The MWCNTs adsorption isotherms fitted slightly better with the Freundlich model than the Langmuir model, suggesting the SAs sorption on MWCNTs may be controlled by the

heterogeneous chemisorption. The Freundlich exponent  $n < 1.0$  represented an advantageous adsorption condition, indicating a favorability of SAs adsorption by MWCNTs. Both the Freundlich and the Langmuir models described the SWCNTs adsorption isotherms very well, suggesting that some heterogeneity on the surfaces or pores of SWCNTs played an important role in SAs adsorption and different sites with several adsorption energies were involved. These results were consistent with the previous works on the adsorption process of SAs by different kinds of CNTs.<sup>30</sup> The general trend of Freundlich affinity coefficient ( $K_f$ ) was  $\text{SPY} > \text{SDZ} > \text{SMX}$  for both MWCNTs and SWCNTs. In experiments conducted with the same adsorbate, the  $K_f$  values in different adsorbent followed the order:  $\text{SWCNTs} > \text{MWCNTs} > \text{sediments}$ , and the maximum adsorption capacities of SAs on SWCNTs were three orders of magnitude higher than MWCNTs. Compared to MWCNTs, SWCNTs had relatively higher specific surface area and thus had higher SAs sorption capacity. Similar conclusion was also made by earlier researchers.<sup>31</sup>

The  $\log K_{ow}$  ( $n$ -octanol–water partitioning coefficients) is a typical hydrophobic parameter of organic chemicals. Compounds with a low  $K_{ow}$  values (less than 10) may be considered to be relatively hydrophilic, therefore they have a property of high solubility in water as well as low adsorption coefficient ( $K_{oc}$ ) in soil and sediment.<sup>43</sup> In this case,  $\log K_{ow}$  of SMX, SPY, and SDZ were 0.9, 0.35 and  $-0.09$  respectively, indicating that they were hydrophilic polar organics.<sup>44</sup> Thus the adsorption capacities of sediments on SAs were low. Colloid-associated transport might likely happen when the sorption capacity of colloid for pollutants was larger than that of soil.<sup>45</sup> As a result, SWCNTs and MWCNTs could change the transport of SAs in sediment due to their preferential sorption on SAs.

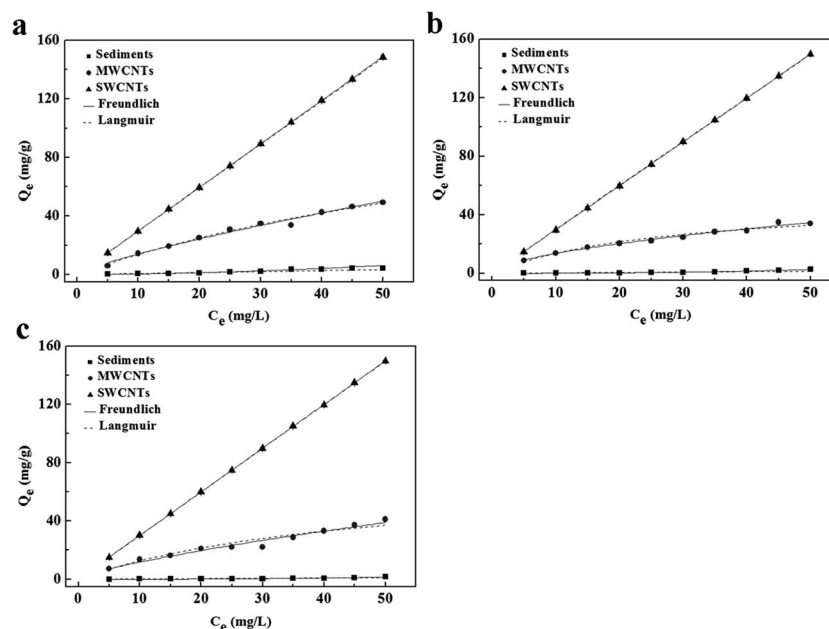


Fig. 3 Measured (dots), Freundlich and Langmuir model fitted (lines) sorption isotherms of SMX (a), SPY (b), and SDZ (c) on sediments, MWCNTs and SWCNTs.

Table 3 Freundlich and Langmuir equation parameters for SAs adsorption by sediments, MWCNTs and SWCNTs

Adsorbate	Adsorbent	Freundlich			Langmuir		
		$K_f$	$n$	$R^2$	$K_L$	$Q_m$	$R^2$
SMX	Sediments	$5.830 \times 10^{-3}$	1.782	0.9668	$4.172 \times 10^{-6}$	$1.609 \times 10^4$	0.7188
	MWCNTs	2.092	0.7299	0.9845	$1.116 \times 10^{-2}$	136.5	0.9811
	SWCNTs	2.972	1.000	1	$1.462 \times 10^{-4}$	$2.039 \times 10^4$	1
SPY	Sediments	$2.204 \times 10^{-4}$	2.400	0.9383	$1.962 \times 10^{-6}$	$1.487 \times 10^4$	0.6193
	MWCNTs	2.974	0.5806	0.9917	372.1	50.43	0.9794
	SWCNTs	3.578	1.001	1	$2.055 \times 10^{-4}$	$1.469 \times 10^4$	1
SDZ	Sediments	$1.877 \times 10^{-4}$	2.300	0.9447	$3.353 \times 10^{-6}$	$7.238 \times 10^3$	0.7435
	MWCNTs	2.261	0.7649	0.98943	$2.081 \times 10^{-2}$	72.43	0.9783
	SWCNTs	2.998	0.9999	1	$6.299 \times 10^{-5}$	$4.768 \times 10^4$	1

### 3.2 Mobility of SAs in sediment columns

It was clearly shown in Fig. 4 that SAs were retained in every layer of the column in low concentrations (about 0.01–0.03 mg g<sup>-1</sup>, except for 0.09 mg g<sup>-1</sup> SMX in the top one layer) and concentrations slightly decreased with the depth of sediment when sediments were the only filler of the column. It suggested that SAs could transport vertically in sediment and were of high mobility. While the addition of both types of CNTs led to increased retention of SAs in sediment, with most retained in top three layers (3 cm). For example, only 2.4% of SPY was retained in sediment while 10.6%, 48.4% of SPY was retained in MWCNTs-S and SWCNTs-S, respectively. This phenomenon might due to the superior adsorption behavior of CNTs on SAs as well as limited transport of both types of CNTs in sediment.<sup>12,31,33,39</sup> The results were also similar to the previous research.<sup>17</sup> However, the retention of all SAs in MWCNTs-S were lower than that in SWCNTs-S, which might due to the stronger

adsorption affinity of SWCNTs (see Table 3). Besides, different retentions of SAs in SWCNTs-S were in the order of: SMX < SDZ < SPY, which followed the same trend of the adsorption affinity coefficient of SWCNTs on them.

Breakthrough curves were also used to indicate the mobility of SAs (Fig. 5). The breakthrough curves were expressed in term of  $C/C_0$  as a function of the number of pore volumes passing through the column, where  $C_0$  is the concentration of inflow,  $C$  is the concentration of outflow. Transport of SAs varied with columns. In sediment columns, SPY and SDZ concentrations in passing through the first pore volume were about 60% of inflow concentrations while it took more leaching time (passing through 2.3 pore volumes and 1.6 pore volumes, respectively) to reach 60% of inflow concentrations in MWCNTs-S columns. Eventually, it also took more leaching time (passing through 5.0 pore volumes and 3.0 pore volumes, respectively) for SPY and SDZ to reach the plateau value in MWCNTs-S columns than in

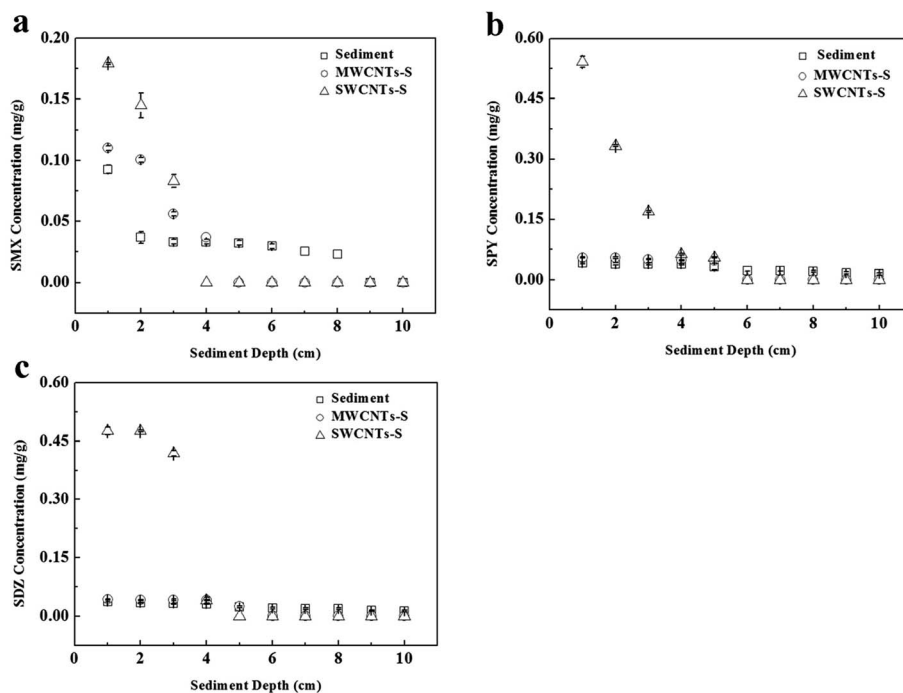


Fig. 4 Concentrations of SMX (a), SPY (b), and SDZ (c) in each layer of different columns. 'Sediment' referred to column with only sediments, 'MWCNTs-S' and 'SWCNTs-S' referred to column with sediments mixed with MWCNTs and SWCNTs, respectively.

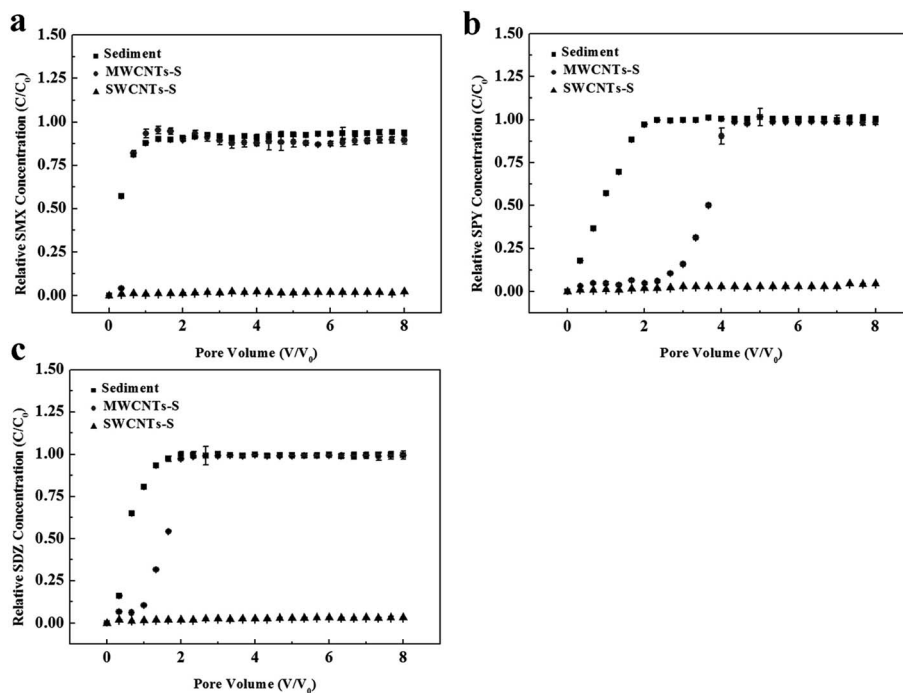


Fig. 5 Breakthrough curves of SMX (a), SPY (b), and SDZ (c) in different columns. 'Sediment' referred to column with only sediments, 'MWCNTs-S' and 'SWCNTs-S' referred to column with sediments mixed with MWCNTs and SWCNTs, respectively.

sediment columns (both passing through 2.0 pore volumes). The results could be reasonably interpreted with the better adsorption property of MWCNTs than that of sediments on SPY and SDZ.<sup>33</sup> Whereas, as for SMX, it tended to increase rapidly

and reached final plateau values ( $C/C_0$ ) of 93.8% and 89.5% in sediment and MWCNTs-S columns respectively. These differences in the trends of curves might due to the different adsorption properties of MWCNTs on different SAs. The

adsorption affinity on SMX was lower than that on SPY and SDZ, so the presence of MWCNTs in sediment did not contribute obviously to the SMX retention. Nevertheless, the phenomenon was extremely distinctive in the SWCNTs-S leaching experiments. SAs almost all retained in the SWCNTs-S with no breakthrough detected. The solution concentrations were 2.2% (SMX), 4.6% (SPY) and 3.3% (SDZ) of inflow concentrations after passing through 8.0 pore volumes, which may due to the relatively high adsorption capacity of SWCNTs on SAs.

In this study, SAs demonstrated good mobility at a relatively high concentration in sediment. The experiments imitated the situation in which SAs solutions flowed at a low velocity in river and on the sediment surface. Reduction of streamflow caused the accumulation of sediment.<sup>46</sup> SAs might leach through the surface or subsurface sediment environment. However, with the presence of CNTs, especially SWCNTs, in sediment, more SAs were retained. But in real sediment environment, such high concentration of CNTs ( $4.8 \text{ mg g}^{-1}$ ) was not common except for those severe contamination spots. Hence it needs some future studies conducting with lower concentration of CNTs in sediment to determine whether it will still decrease the mobility of SAs or not.

### 3.3 Transportation of SAs associated with CNTs through sediment columns

It can be seen in Fig. 6 that SAs were mostly retained in top three layers (3 cm) when associated with CNTs. It suggested that SAs associated with CNTs could transport vertically in sediment but CNTs limited the transport of SAs. Clogged MWCNTs and SWCNTs were visible on the sediment surface and subsurface (top two layers), and these CNTs might contribute to the

retention of SAs. Zeta potentials of CNTs and sediments were negative, thus the attachment between them was unfavorable according to the classical Derjaguin–Landau–Verwey–Overbeek (DLVO) theory.<sup>18</sup> Nonetheless, the surfaces of sediments grains were usually heterogeneous with both negative and positive sites and the positive or less negative sites on them would be favorable for CNTs deposition.<sup>18,47</sup> In general, the retention of all SAs increased compared to the corresponding experiments with CNTs-mix sediment. SAs were retained more in the first layer when the mixture in inflow had not reached equilibrium than that had reached equilibrium in advance. These phenomena might result from the difference in reaction time between SAs and CNTs. Furthermore, SWCNTs retained more SAs in sediment than MWCNTs did whether the mixture in inflow had reached equilibrium in advance or not. For instance, for SMX, average retention masses in the first layer were as follows: MWCNTs-nonequilibrium (0.31 mg) < MWCNTs-equilibrium (0.54 mg) < SWCNTs-nonequilibrium (0.69 mg) < SWCNTs-equilibrium (0.72 mg). These phenomena might be related to the adsorption–desorption dynamic equilibrium, but further studies are still needed for verification. As for the different adsorbates, retention capacities of SMX, SPY and SDZ also followed the same order as the adsorption affinity of CNTs on them (SMX < SDZ < SPY).

As shown in Fig. 7, with the absence of CNTs in the inflow, significant breakthroughs of SAs were observed after solutions passing through only 1–2 pore volumes. Besides, with MWCNTs added in the inflow, whether the mixture had reached equilibrium in advance or not, the breakthrough curves were nearly coincided with the previous one (*i.e.* no CNTs in the inflow), except for the SMX-nonequilibrium breakthrough curve. It

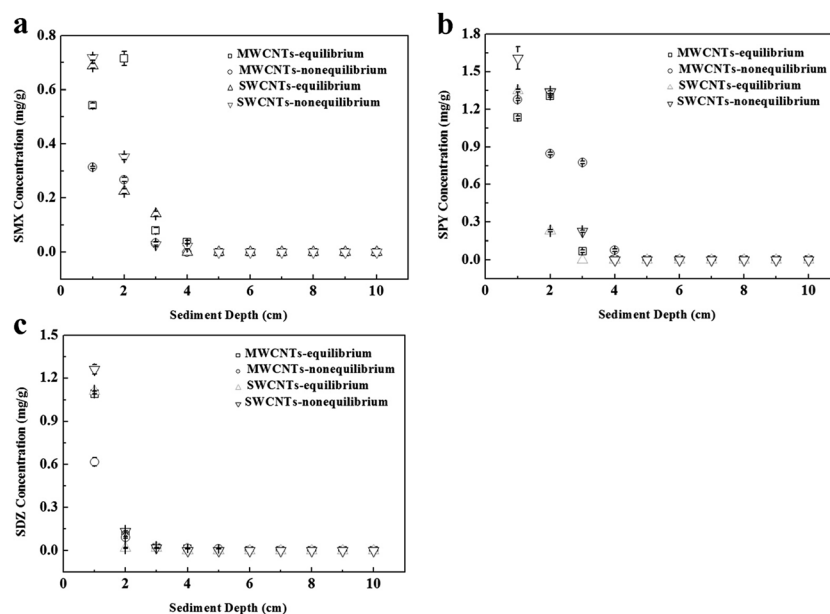


Fig. 6 Concentrations of SMX (a), SPY (b), and SDZ (c) in each layer of columns with different inflows. 'MWCNTs-equilibrium' referred to inflow with MWCNTs and SAs that had reached equilibrium in advance, 'MWCNTs-nonequilibrium' referred to inflow with MWCNTs and SAs that had not reached equilibrium, 'SWCNTs-equilibrium' referred to inflow with SWCNTs and SAs that had reached equilibrium in advance, and 'SWCNTs-nonequilibrium' referred to inflow with SWCNTs and SAs that had not reached equilibrium.



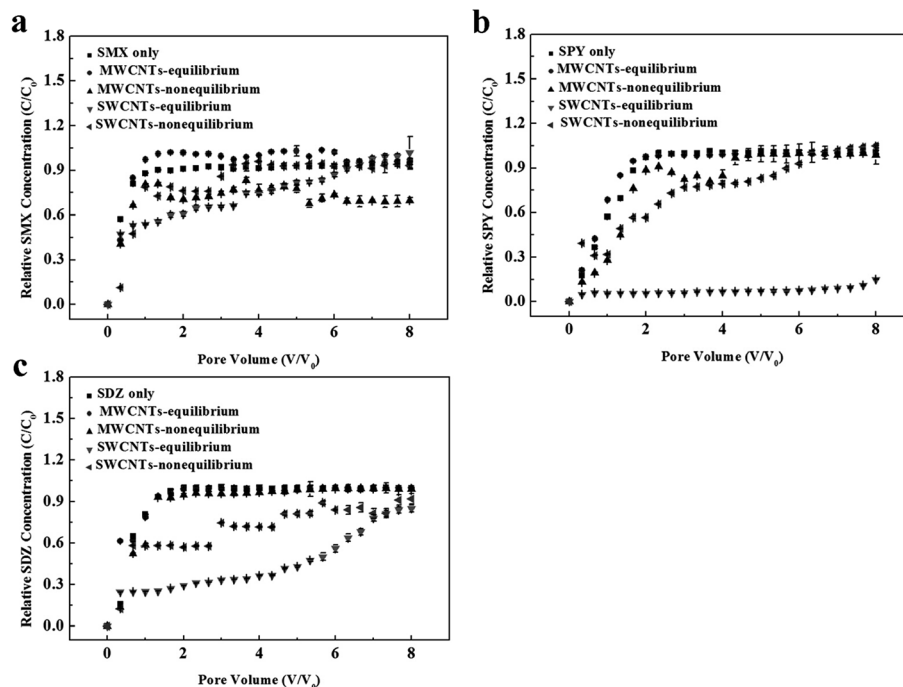


Fig. 7 Breakthrough curves of SMX (a), SPY (b), and SDZ (c) with different inflows. 'SMX only', 'SPY only' and 'SDZ only' referred to inflow with only SMX, SPY and SDZ, respectively. 'MWCNTs-equilibrium' referred to inflow with MWCNTs and SAs that had reached equilibrium in advance, 'MWCNTs-nonequilibrium' referred to inflow with MWCNTs and SAs that had not reached equilibrium, 'SWCNTs-equilibrium' referred to inflow with SWCNTs and SAs that had reached equilibrium in advance, and 'SWCNTs-nonequilibrium' referred to inflow with SWCNTs and SAs that had not reached equilibrium.

reached final concentration plateaus in a lower concentration (75% of inflow). However, when SWCNTs was added in the inflow (adsorption equilibrium of SAs to SWCNTs was reached in advance), the SAs concentrations were gradually increased with the further increase of pore volumes before it reached the final concentration plateaus. The SMX curve was the first one to reach final concentration plateaus, followed by the SDZ curve. It was worth nothing that the SPY curve finally reached the concentrations in 98% of inflow concentration after passing through 22 pore volumes (data not shown). Nevertheless, when the SAs-SWCNTs mixture had not reached adsorption equilibrium in advance, the breakthrough curves of SAs increased sharply before passing through 1 pore volume and then slowly grew until reached the final concentration plateaus (about 95% of inflow) after passing through 4–8 pore volumes. Breakthrough curve of SMX in SAs-SWCNTs nonequilibrium experiments firstly reached the final concentration plateaus, with subsequent SDZ and followed by SPY. The differences were also likely on account of the differences in SWCNTs adsorption capacities and adsorption-desorption dynamic equilibrium among three kinds of SAs. These results indicated that CNTs in inflow could markedly limit SAs transport.

In the absence of CNTs, the transport of SAs in columns were impeded by the sorption to sediments, indicated by the retardation factor,  $R$ :<sup>48</sup>

$$R = 1 + \frac{\rho_b}{\theta} K_d \quad (4)$$

where  $\rho_b$  ( $\text{g cm}^{-3}$ ) and  $\theta$  (unitless) are the bulk density and porosity of the soil column and  $K_d$  ( $\text{L kg}^{-1}$ ) is the distribution coefficient between the sediments and solution. In the presence of CNTs, the retardation could also be referred to the common equation used to describe facilitated transport of nonionic hydrophobic organic compounds by DOM:<sup>49</sup>

$$R = 1 + \frac{\rho_b}{\theta} \left( \frac{K_d}{1 + K_{\text{DOM}} C_{\text{DOM}}} \right) \quad (5)$$

where  $K_{\text{DOM}}$  ( $\text{L kg}^{-1}$ ) is the partition coefficient of a compound to DOM (or CNTs in this case) and  $C_{\text{DOM}}$  ( $\text{kg L}^{-1}$ ) is the concentration of DOM (or CNTs in this case).

The  $K_d$  values and  $K_{\text{DOM}}$  values were calculated according to Fig. 8. The  $R$  values calculated from the formula (4) and formula (5) were listed in Table 4. In the absence of CNTs, the  $R$  values of SMX, SPY, and SDZ were very close to 1 because of the low adsorption capacities of sediments on SAs, and as a result, the sediment would have little effect on SAs transport. Thus it was in line with expectation that SAs broke through after only passing through 1–2 pore volumes in sediment columns. The  $R$  values of SMX, SPY, and SDZ in the presence of MWCNTs were 127.19, 61.14, and 36.46, respectively while the  $R$  values of SMX, SPY, and SDZ with the presence of SWCNTs were 86.83, 39.01, and 23.70, respectively. The  $R$  values showed that the CNTs could absorb a part of SAs, leading to a retardation or nonoccurrence of the breakthrough of SAs in sediment, which also theoretically proved the experiments results. But the calculated  $R$  values of SAs were lower in the presence of SWCNTs than with

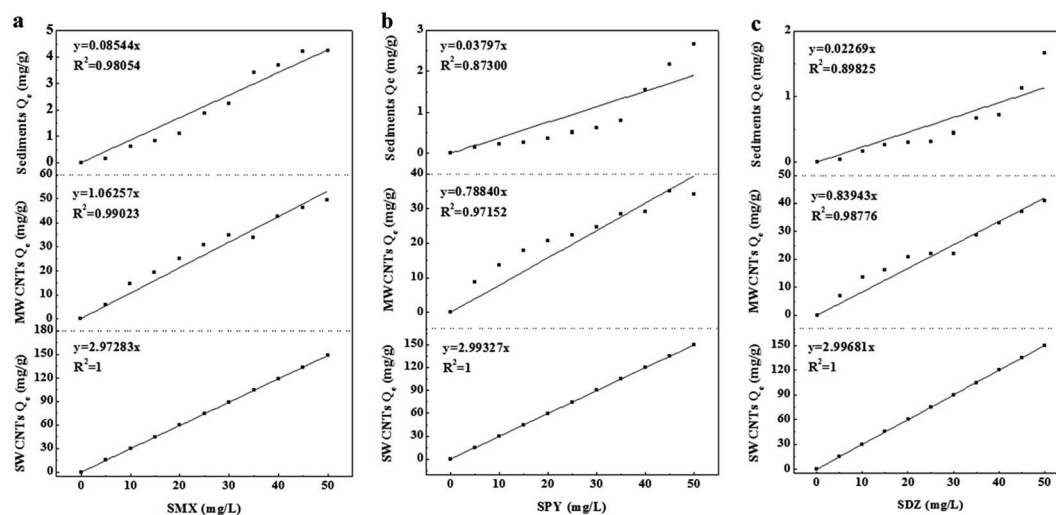


Fig. 8 Sorption isotherms of SMX (a), SPY (b) and SDZ (c) to sediments, MWCNTs, and SWCNTs.

**Table 4** The distribution coefficient ( $K_d$ ), the partition coefficient to DOM (or CNTs in this case) ( $K_{\text{DOM}}$ ), and the retardation factor ( $R$ ) for SMX, SPY and SDZ<sup>a</sup>

Adsorbate	SMX	SPY	SDZ
$K_d$ (L kg <sup>-1</sup> )	85.44	37.97	22.69
MWCNTs $K_{\text{DOM}}$ (L kg <sup>-1</sup> )	1062.57	788.40	839.43
SWCNTs $K_{\text{DOM}}$ (L kg <sup>-1</sup> )	2972.83	2993.27	2996.81
$R$	1.17	1.08	1.05
MWCNTs $R'$	127.19	61.14	36.46
SWCNTs $R'$	86.83	39.01	23.70

<sup>a</sup> Calculated using  $\rho_b = 1.11$  (g cm<sup>-3</sup>),  $\theta = 0.55$  and  $C_{\text{DOM}} = 0.33 \times 10^{-3}$  (kg L<sup>-1</sup>).

the presence of MWCNTs, indicating an opposite result to the real experiments. Therefore, the different effects between CNTs and DOM on SAs breakthrough suggested that the CNTs could influence the transport of SAs in different mechanisms from DOM. As a result, more studies are needed to further understand the mechanisms of CNTs affecting the mobility of SAs.

## 4. Conclusion

The SAs are of high mobility in sediment due to the low adsorption capacity of sediments to them. However, findings in this study indicated that CNTs could limit the mobility of SAs in sediment and such an impact was affected by adsorption affinity. With the presence of CNTs, especially SWCNTs in sediment, SAs had limited mobility in the sediment column even at a high concentration in inflow. Moreover, with an addition of CNTs in inflow, SAs showed low mobility due to the strong retardation effect induced by the adsorption of CNTs. This CNTs-associated effect should be taken into account when evaluating the potential environmental risks of SAs. Nevertheless, considering the different types of CNTs from different manufacturers, the different sediment environments, and various bioavailability processes in sediment, further studies on

the transport mechanisms of CNTs and SAs in sediment media are of great importance for better understanding the behavior and fate of CNTs and SAs in the natural sediment environment.

## Acknowledgements

The authors are grateful for the financial supports from National Natural Science Foundation of China (51521006, 51579095, and 51378190), the Program for Changjiang Scholars and Innovative Research Team in University (IRT-13R17), Hunan province university innovation platform open fund project (14K020), the Interdisciplinary Research Funds for Hunan University, the Scientific Research Foundation for the Returned Overseas Chinese Scholars, State Education Ministry and the International S&T Cooperation Program of China (2015DFG92750).

## References

- 1 S. Iijima, *Nature*, 1991, **354**, 56–58.
- 2 M. S. Mauter and M. Elimelech, *Environ. Sci. Technol.*, 2008, **42**, 5843–5859.
- 3 M. M. Barsan, M. E. Ghica and C. M. A. Brett, *Anal. Chim. Acta*, 2015, **881**, 1–23.
- 4 C. L. Li, A. Schäffer, J.-M. Séquaris, K. László, A. Tóth, E. Tombácz, H. Vereecken, R. Ji and E. Klumpp, *J. Colloid Interface Sci.*, 2012, **377**, 342–346.
- 5 W. W. Tang, G. M. Zeng, J. L. Gong, Y. Liu, X. Y. Wang, Y. Y. Liu, Z. F. Liu, L. Chen, X. R. Zhang and D. Z. Tu, *Chem. Eng. J.*, 2012, **211–212**, 470–478.
- 6 F. Yu, S. Sun, S. Han, J. Zheng and J. Ma, *Chem. Eng. J.*, 2016, **285**, 588–595.
- 7 S. Boncel, J. Kyziol-Komosinska, I. Krzyzewska and J. Czupiol, *Chemosphere*, 2015, **136**, 211–221.
- 8 F. X. Wang, S. Y. Xiao, Y. Y. Hou, C. L. Hu, L. L. Liu and Y. P. Wu, *RSC Adv.*, 2013, **3**, 13059–13084.
- 9 A. B. Sulong and J. Park, *J. Compos. Mater.*, 2010, **45**, 931–941.

- 10 B. Nowack and T. D. Bucheli, *Environ. Pollut.*, 2007, **150**, 5–22.
- 11 A. R. Köhler, C. Som, A. Helland and F. Gottschalk, *J. Cleaner Prod.*, 2008, **16**, 927–937.
- 12 D. Kasel, S. A. Bradford, J. Simunek, T. Putz, H. Vereecken and E. Klumpp, *Environ. Pollut.*, 2013, **180**, 152–158.
- 13 S. Li, T. A. Anderson, M. J. Green, J. D. Maul and J. E. Canas-Carrell, *Environ. Sci.: Processes Impacts*, 2013, **15**, 1130–1136.
- 14 T. Hofmann and F. von der Kammer, *Environ. Pollut.*, 2009, **157**, 1117–1126.
- 15 X. T. Wang, L. Cai, P. Han, D. H. Lin, H. Kim and M. P. Tong, *Environ. Pollut.*, 2014, **195**, 31–38.
- 16 Y. Y. Lu, K. Yang and D. H. Lin, *Environ. Pollut.*, 2014, **192**, 36–43.
- 17 S. Li, U. Turaga, B. Shrestha, T. A. Anderson, S. S. Ramkumar, M. J. Green, S. Das and J. E. Canas-Carrell, *Ecotoxicol. Environ. Saf.*, 2013, **96**, 168–174.
- 18 J. Fang, X. Q. Shan, B. Wen and R. X. Huang, *Geoderma*, 2013, **207–208**, 1–7.
- 19 J. L. Martinez, *Environ. Pollut.*, 2009, **157**, 2893–2902.
- 20 G. Hamscher, S. Sczesny, H. Hoper and H. Nau, *Anal. Chem.*, 2002, **74**, 1509–1518.
- 21 W. Baran, E. Adamek, J. Ziemianska and A. Sobczak, *J. Hazard. Mater.*, 2011, **196**, 1–15.
- 22 H. T. T. Thuy and T. T. C. Loan, *Environ. Sci. Pollut. Res.*, 2011, **18**, 835–841.
- 23 M. Unold, R. Kasteel, J. Groeneweg and H. Vereecken, *J. Contam. Hydrol.*, 2009, **103**, 38–47.
- 24 B. A. Lalonde, W. Ernst and L. Greenwood, *Bull. Environ. Contam. Toxicol.*, 2012, **89**, 547–550.
- 25 X. M. Liang, B. W. Chen, X. P. Nie, Z. Shi, X. P. Huang and X. D. Li, *Chemosphere*, 2013, **92**, 1410–1416.
- 26 S. Bergeron, R. Boopathy, R. Nathaniel, A. Corbin and G. LaFleur, *Int. Biodeterior. Biodegrad.*, 2015, **102**, 370–374.
- 27 A. Gobel, A. Thomsen, C. S. Mc Ardell, A. Joss and W. Giger, *Environ. Sci. Technol.*, 2005, **39**, 3981–3989.
- 28 Z. H. Lu, G. S. Na, H. Gao, L. J. Wang, C. G. Bao and Z. W. Yao, *Sci. Total Environ.*, 2015, **527**, 429–438.
- 29 Y. Tian, B. Gao, V. L. Morales, H. Chen, Y. Wang and H. Li, *Chemosphere*, 2013, **90**, 2597–2605.
- 30 H. Kim, Y. S. Hwang and V. K. Sharma, *Chem. Eng. J.*, 2014, **255**, 23–27.
- 31 X. Zhang, B. Pan, K. Yang, D. Zhang and J. Hou, *J. Environ. Sci. Health, Part A: Toxic/Hazard. Subst. Environ. Eng.*, 2010, **45**, 1625–1634.
- 32 D. Zhang, B. Pan, M. Wu, B. Wang, H. Zhang, H. B. Peng, D. Wu and P. Ning, *Environ. Pollut.*, 2011, **159**, 2616–2621.
- 33 L. L. Ji, W. Chen, S. R. Zheng, Z. Y. Xu and D. Q. Zhu, *Langmuir*, 2009, **25**, 11608–11613.
- 34 B. Pan, D. Zhang, H. Li, M. Wu, Z. Y. Wang and B. S. Xing, *Environ. Sci. Technol.*, 2013, **47**, 7722–7728.
- 35 D. W. Nelson and L. E. Sommers, *Proc. Indiana Acad. Sci.*, 1974, **84**, 456–462.
- 36 W. H. Hendershot and M. Duquette, *Soil Sci. Soc. Am. J.*, 1986, **50**, 605–608.
- 37 B. Liang, J. Lehmann, D. Solomon, J. Kinyangi, J. Grossman, B. O'Neill, J. O. Skjemstad, J. Thies, F. J. Luizao, J. Petersen and E. G. Neves, *Soil Sci. Soc. Am. J.*, 2006, **70**, 1719–1730.
- 38 W. H. Patrick, *Soil Sci. Soc. Am. J.*, 1958, **22**, 366–367.
- 39 D. P. Jaisi and M. Elimelech, *Environ. Sci. Technol.*, 2009, **43**, 9161–9166.
- 40 U. S. E. P. A., EPA Method 1694, 2007, EPA 821-R-08-002.
- 41 S. Thiele-Bruhn, T. Seibicke, H. R. Schulten and P. Leinweber, *J. Environ. Qual.*, 2004, **33**, 1331–1342.
- 42 F. Lian, B. B. Sun, X. Chen, L. Y. Zhu, Z. Q. Liu and B. S. Xing, *Environ. Pollut.*, 2015, **204**, 306–312.
- 43 J. De Bruijn, F. Busser, W. Seinen and J. Hermens, *Environ. Toxicol. Chem.*, 1989, **8**, 499–512.
- 44 M. S. Diaz-Cruz, M. J. L. de Alda and D. Barcelo, *J. Chromatogr. A*, 2006, **1130**, 72–82.
- 45 A. D. Karathanasis, *Soil Sci. Soc. Am. J.*, 1999, **63**, 830–838.
- 46 G. M. Zeng, M. Chen and Z. T. Zeng, *Nature*, 2013, **499**, 154.
- 47 D. Bouchard, W. Zhang, T. Powell and U. S. Rattanadompol, *Environ. Sci. Technol.*, 2012, **46**, 4458–4465.
- 48 A. T. Kan and M. B. Tomson, *Environ. Toxicol. Chem.*, 1990, **9**, 253–263.
- 49 L. L. Zhang, L. L. Wang, P. Zhang, A. T. Kan, W. Chen and M. B. Tomson, *Environ. Sci. Technol.*, 2011, **45**, 1341–1348.